Mon. Not. R. astr. Soc. (1981) **197**, 325–337

A statistical study of flat-spectrum radio sources at 966 MHz

P. K. Moore, I. W. A. Browne, E. J. Daintree, R. G. Noble and D. Walsh *University of Manchester, Nuffield Radio Astronomy Laboratories, Jodrell Bank, Macclesfield, Cheshire SK11 9DL*

Received 1981 February 23; in original form 1980 December 22

Summary. A sample of 36 flat-spectrum radio sources has been observed at 966 MHz with a resolution of ~0.5 arcsec. Sixty-seven per cent of them showed evidence of extended emission several arcsec from an unresolved nucleus. Typically this emission constitutes 10 per cent of the total flux at 1 GHz. Our results show that most of the sources have asymmetric double structure. Interpreting this in terms of the relativistic jet model requires bulk relativistic motions up to several hundred kpc from the nucleus. The ratio of flux from the extended component to that from the nucleus is compared with what is expected from the model and found to be in rough quantitative agreement. The presence of extended emission, variability and spectral type are found to be correlated, and possible explanations for this are sought in terms of the relativistic jet model.

1 Introduction

Recent observations of flat-spectrum radio sources have indicated that they may not be as compact as has been previously supposed. The results of Conway & Stannard (1975), Davis, Stannard & Conway (1977), Perley & Johnston (1979), and Perley, Fomalont & Johnston (1980) have indicated the presence of significant amounts of extended emission surrounding the nuclei of these sources. In order to study this further a complete sample of flat-spectrum sources has been observed at 966 MHz with high angular resolution. The results are used to attempt to answer the following three questions:

(i) How common is extended emission around flat-spectrum sources?
(ii) What is the morphology of those sources which show extended emission?
(iii) Are the results compatible with the relativistic jet model of Scheuer & Readhead (1979) and Blandford & Königl (1979)?

Question (ii) is only considered briefly here, further discussion being deferred to a later paper (Paper II – Moore, in preparation).

The sample of flat-spectrum sources was selected from the Jodrell Bank 966-MHz survey (Cohen *et al.* 1977; Porcas *et al.* 1980) using the following criteria: $40° < \delta < 70°$; $|b| > 10°$; $S_{966} \geqslant 1$ Jy; $\alpha_1^3 > -0.5$, where α_1^3 is the mean spectral index between 1 and 3 GHz defined in the sense $S \propto \nu^{\alpha}$. Several sources in the original survey suffered from confusion and some additional observations were made with a 900 λ-baseline interferometer to measure reliable 966-MHz flux densities for such sources. The final sample of 36 sources is listed in Table 1 together with flux densities and optical identifications.

2. Observations and data reduction

The Jodrell Bank Mk II-Defford interferometer was used at 966 MHz in 1978 March and June to search for extended emission around all the sources in the sample. The frequency

Table 1. Observed properties of sources in the complete sample. S_{966} is the 966-MHz flux density in Jy, ID the optical identification using the nomenclature of Cohen *et al.* (1977), P the probability of a source being unresolved, and r the ratio of the flux density of extended component to that of the nucleus.

Source	S_{966}	ID	P	r
0133 + 476	1.54	BSO	1.000	<0.080
0316 + 413	15.03	GCL	0.000	0.039
0600 + 442	1.19	(E)	0.000	1.071
0609 + 607	1.25	BSO	0.445	<0.080
0642 + 449	1.30	QSO	0.408	<0.080
0707 + 476	1.10	NI	0.122	<0.080
0710 + 439	1.33	RO	0.102	<0.080
0814 + 425	2.46	QSO	0.042	0.095★
0820 + 560	1.57	QSO	0.831	<0.080
0828 + 493	1.23	BSO	0.002	0.114★
0831 + 557	8.42	GCL	0.000	0.355
0850 + 581	1.12	QSO	0.018	0.096
0859 + 470	2.36	QSO	0.000	0.153
0900 + 428	1.52	GCL	0.000	0.145
0945 + 408	2.14	QSO	0.000	0.182★
0954 + 556	3.78	QSO	0.000	0.161★
1031 + 567	2.30	(RO)	0.999	<0.080
1150 + 497	2.11	QSO	0.000	0.273
1415 + 463	1.11	QSO	0.001	0.255
1418 + 546	1.20	QSO	0.267	<0.080
1427 + 543	1.05	BSO	0.000	0.165
1624 + 416	2.23	E	0.874	<0.080
1636 + 473	1.13	QSO	0.209	1.333
1642 + 690	1.55	BSO	0.000	0.215
1656 + 482	1.05	RO	0.000	0.212
1656 + 571	1.00	QSO	0.002	3.063
1738 + 476	1.14	BSO	0.357	<0.080
1739 + 522	2.01	QSO	0.000	0.132
1749 + 701	1.98	QSO	0.954	<0.080
1800 + 440	1.01	QSO	0.000	0.304
1807 + 698	2.87	G	0.000	0.245
1823 + 568	1.33	QSO	0.000	0.333
1954 + 513	2.36	QSO	0.000	0.156
2200 + 420	4.00	QSO	0.749	<0.080
2351 + 456	2.09	RO	0.000	0.159
2352 + 495	2.78	G	0.000	0.020

was chosen as a compromise between the conflicting requirements of resolution and of sensitivity to the extended emission which is likely to have a steep spectrum (Davis *et al.* 1977). Since total flux densities at 966 MHz were available, the use of this frequency had the additional advantage that visibilities could be measured. The interferometer has a baseline of 127 km, giving it a minimum lobe spacing of 0.5 arcsec at 966 MHz.

Each source was observed for a minimum of 5 hr, and those showing clear evidence of structure for an appreciably longer time (see Paper II). The amplitudes were calibrated by assuming a flux density of 2.59 Jy for 2003 − 025, which puts the flux densities on the scale of Baars *et al.* (1977).

The phase stability of the interferometer was poor, due to atmospheric variations above each telescope and in the radio-link path. This, together with the limited aperture-plane coverage of a single baseline, makes analysis by Fourier transform techniques difficult. Since, at this stage, we only require knowledge of whether a source is resolved or not, it is sufficient to test the fringe amplitudes by comparing them with the constant value expected for an unresolved source. A χ^2 test was used for this purpose, the method being similar to that described by Kesteven, Bridle & Brandie (1976). The results in the fourth column of Table 1 give the probability of the data being consistent with constant amplitude. The same procedure was applied to the calibration source 2003 − 025, and the probability of its being unresolved found to be 0.55, confirming that it may be treated as a point source.

In determining where to draw the line between resolved and unresolved sources, two effects need to be borne in mind. First there were occasional instrumental difficulties, such as a telescope drifting off-source, which reduced the recorded amplitude. Most of these occurrences were noted and the relevant section removed from the data but it is possible that a few remain and they would tend to make an unresolved source appear resolved. Second, because of the limited aperture-plane coverage of the observations, some extended emission may have been missed. It was decided to set the level of significance for distinguishing resolved from unresolved sources at 5 per cent, but it should be noted that there are very few borderline sources and the results which follow are affected very little by changes in this threshold level.

The maximum visibility of each source was calculated by comparing the maximum observed interferometer amplitude with the total flux density measured during the original survey (Cohen *et al.* 1977). Unresolved sources tended to have higher visibilities than resolved ones, as expected, but there were two unresolved sources with anomalously low visibilities. One of them − 1636 + 473 − has been observed by Porcas *et al.* (1980) who find extended emission about 19 arcsec away from a compact nucleus. This emission was missed due to the poor aperture-plane coverage of our observations. This source is therefore classified as resolved and it will be discussed further in Paper II. The other unresolved source with low visibility is 1418 + 546, but there is evidence to suggest that this source is highly variable (see Section 7).

3 Results

One result follows immediately from these observations, and that is that 24 out of 36, i.e. 67 per cent, of flat-spectrum sources selected at 966 MHz have significant amounts of extended emission with an angular size greater than 0.1 arcsec. Although this is the first time that a study has been made of a complete sample of such sources, the results do seem to be in rough agreement with earlier studies. In particular, Perley *et al.* (1980) suggest that 30 to 40 per cent of compact sources exhibit low-brightness extended features having steep spectra. The larger number of extended sources found in our observations can be

Table 2. The number of resolved sources found in each of three optical identification categories.

	Resolved	
	Yes	No
Quasar (QSO and BSO)	16	8
Galaxy (G, GCL and RO)	7	2
Other (E and NI)	1	2

explained by the lower frequency used, resulting in the extended components being relatively stronger. Similar proportions of resolved sources have also been reported by Weiler & Johnston (1980) and Wardle (1978) amongst flat-spectrum BL Lac objects.

The only observations in apparent disagreement with our results are those of Bentley *et al.* (1976), who found virtually no extended flat-spectrum quasars in the Parkes sample of sources. Their observing procedure, however, consisted of a few short tracks with a single-baseline interferometer at widely spaced hour-angles. This appears to be a far less sensitive test for extended emission than the long tracks and χ^2 test used here. Some more recent observations (Bentley, private communication) show that many of these sources are indeed resolved.

Table 2 shows the results broken down into different identification classes. A χ^2 test shows that the probability of the three classes having the same fraction of resolved sources is 37 per cent. Extended emission appears to be common among both galaxies and quasars with flat spectra.

4 The relativistic jet model

In addition to the χ^2 test described previously, the data on all of the resolved sources were analysed by model fitting to the fringe amplitudes. A description of this technique and the detailed results for individual sources are presented in Paper II, together with some results at frequencies other than 966 MHz. We shall, however, use the results of the 966-MHz model-fitting here, in an attempt to explain some of the statistical properties of our sample of flat-spectrum sources.

It was found that almost all of the sources could be represented approximately by a model consisting of two components, one of which was compact and consequently unresolved in our observations, the other being extended and resolved. No source was found with extended emission on both sides of the nucleus as occurs typically with steep-spectrum sources (e.g. Jenkins, Pooley & Riley 1977). Perley *et al.* (1980) with the VLA and Browne *et al.* (in preparation) with the MTRLI have mapped several flat-spectrum sources. They both find that these sources are asymmetric, often consisting of a compact core and well-defined jet. For those sources in common with our sample there is excellent agreement between the maps and our single-baseline results.

An obvious way to interpret the one-sided or D2 (Miley 1971) structure of flat-spectrum sources is provided by the relativistic jet model of Scheuer & Readhead (1979) and Blandford & Königl (1979). In this model the emission comes from regions with bulk relativistic motions. The nucleus and approaching extended component will be seen due to their Doppler-

boosted flux density, while any receding components will be swamped and not detected. If the velocities involved are sufficiently relativistic then sources will be observed with preferred orientations (Scheuer & Readhead 1979) and many D2 sources will be seen. It is unlikely that the extended components detected here are the counterparts of hot spots in classical double sources (D1 – Miley 1971) due to this requirement of bulk relativistic motions. Estimates of the expansion velocities in D1 sources suggest that these are not large enough for sufficient flux density enhancement to occur (Longair & Riley 1979; Banhatti 1980; Gopal-Krishna 1980). It is more likely that we are seeing emission from the jets which power the outer hotspots such as those seen in NGC 6251 (Waggett, Warner & Baldwin 1977) and 4C 32.69 (Potash & Wardle 1980). It is not clear what the velocities are in these jets, but if the jet in 4C 32.69 is free, Potash & Wardle (1980) suggest a flow velocity $v > 8 \times 10^9$ cm s^{-1}. Velocities of this magnitude may be great enough to produce sufficient flux enhancement to explain the D2 structure, and possibly even enough to outshine the outer hot-spots. This possibility is discussed further by Browne *et al.* (in preparation).

A quantity which we now have available from our amplitude model-fitting for each of the 36 sources is the flux density ratio, r, of the extended component to the nucleus at 966 MHz. It is also possible to make quantitative predictions of the distribution of this quantity from the relativistic jet model. Comparison of the predictions with observation enables the model to be tested, and some constraints put upon its parameters.

5 Theory

In order to try to interpret our observations we consider a highly simplified model of flat-spectrum sources consisting of two oppositely directed relativistic jets. Each of these jets is allowed to radiate from two regions – the nucleus and an outer extended 'jet' component. We shall distinguish these two components by the subscripts n and e respectively. We use the model to predict the results of observing a flux-limited sample of randomly orientated sources with similar properties. Since the jets are relativistic, the imposition of a flux-density limit means that their projection angles to the line of sight are not randomly distributed. Sources will tend to be seen with their jets near to the line of sight, due to relativistic beaming. Consequently only the approaching jet will be visible, resulting in the asymmetric double structure which we observed.

The 966-MHz observations indicated that, at the selection frequency of the sample, the nuclei of these sources dominate. Let us therefore consider a sample of sources selected solely on the basis of their nuclear flux. If the jet velocity in the nucleus is $c\beta_n$ at an angle θ_n to the line of sight, then the observed flux of the nucleus is

$$S = S_t(1 - \beta_n \cos\theta_n)^{\alpha_n - 2}, \tag{1}$$

where S_t is the flux that would be measured transverse to the jet and α_n the spectral index of the nucleus. We follow Scheuer & Readhead (1979) and use an exponent of $(\alpha_n - 2)$. The density of sources in the S, $\cos\theta_n$ plane is thus (Scheuer & Readhead 1979)

$$dN = KS_t^{\delta-1}\, dS_t d(\cos\theta_n),$$

where δ is the slope of the integrated source counts when selected by a non-beamed property (e.g. optical flux). Using equation (1)

$$dN = KS^{\delta-1}(1 - \beta_n \cos\theta_n)^{\delta(2-\alpha_n)} dS d(\cos\theta_n).$$

Integrating over $S > S_R$, i.e. a radio flux limit, and putting in a value of $\delta = -1.5$ gives the

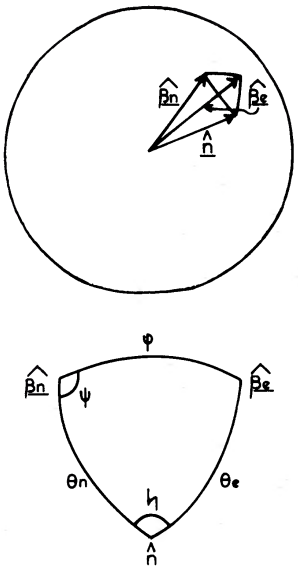

Figure 1. The geometry of the model used. β_n and β_e are the jet velocities in the nucleus and extended component respectively, with angles θ_n and θ_e to the line of sight. ϕ is the intrinsic misalignment of β_n and β_e and η the misalignment in the observer's frame. ψ is the azimuthal angle used to define the direction of β_e.

distribution function for θ_n:

$$f(\theta_n)d\theta_n \propto (1-\beta_n \cos\theta_n)^{-1.5(2-\alpha_n)} \sin\theta_n d\theta_n .$$

For the case $\alpha_n = 0$ this becomes

$$f(\theta_n)d\theta_n = \frac{2(1-\beta_n)^2}{(2-\beta_n)} (1-\beta_n \cos\theta_n)^{-3} \sin\theta_n d\theta_n \tag{2}$$

when normalized over the range 0 to $\pi/2$. This function is plotted in Fig. 2 for three values of the Lorentz factor γ_n. For a given γ_n, the most likely value of θ_n is

$$\theta_n \approx \frac{1}{\sqrt{5}\gamma_n}.$$

The value of r can be calculated from equation (1)

$$r = r_t \frac{(1-\beta_n \cos\theta_n)^{2-\alpha_n}}{(1-\beta_e \cos\theta_e)^{2-\alpha_e}},$$

where r_t is the ratio observed when transverse to both jets. This allows for the possibility that β_n and β_e are not colinear, but are misaligned by an angle ϕ as shown in Fig. 1. There is evidence for such misalignment in several sources observed with VLBI (e.g. Readhead *et al.* 1979). From Fig. 1

$$\cos\theta_e = \cos\theta_n \cos\phi + \sin\theta_n \sin\phi \cos\psi .$$

Thus

$$\frac{r}{r_t} = \frac{(1-\beta_n \cos\theta_n)^{2-\alpha_n}}{(1-\beta_e |\cos\theta_n \cos\phi + \sin\theta_n \sin\phi \cos\psi|)^{2-\alpha_e}}, \tag{3}$$

where the modulus ensures that the ratio is for the approaching component rather than

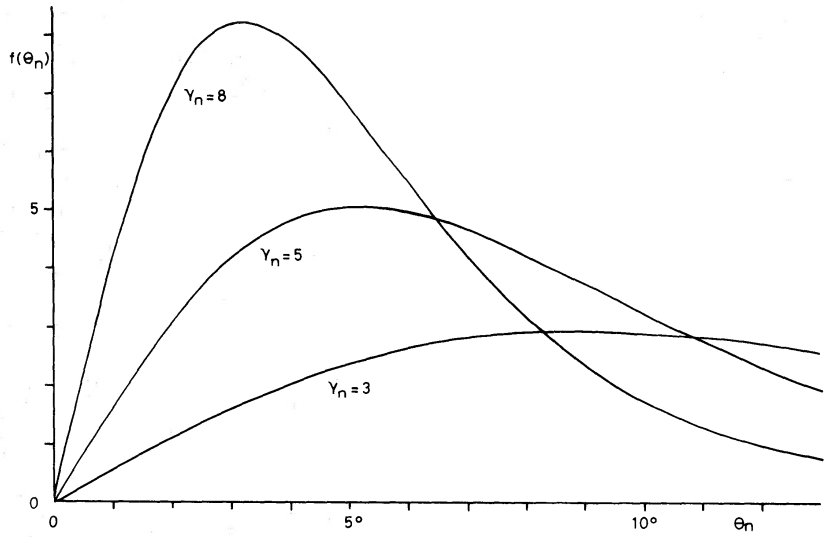

Figure 2. The probability distribution for θ_n, the angle between the nuclear jet and the line of sight, for three values of the Lorentz factor γ_n calculated from equation (2).

the receding one. Strictly this is only true if the two jets on each side of the nucleus have 'S-shaped' symmetry. In practice, however, this has very little influence on our results, since it is only significant for large values of θ_n which are very unlikely to occur in a flux-limited sample (see Fig. 2). Since the sources have been selected by their nuclear flux, the azimuthal angle, ψ, will be uniformly distributed between 0 and 2π, and will be independent of θ_n. Thus the value of r depends on r_t, β_n, β_e, ϕ, α_n and α_e, and there will be a spread of values due to the distributions of θ_n and ψ.

In practice, not all of the six parameters which describe this model are free. α_n and α_e are fixed by direct observation, and typical values of 0 and -1 were used respectively. The resulting model thus had four free parameters, r_t, β_n, β_e and ϕ. Numerical integration over the distributions of θ_n and ψ enabled the distribution of r, $p(r)$ to be calculated using equations (2) and (3).

6 Comparison of model with observation

As they stand, the sources in Table 1 do not form a statistically complete sample selected by the strengths of their nuclear emission alone. To construct such a sample we take those sources in Table 1 with nuclei stronger than 1 Jy and add to them any steep-spectrum sources from the 966-MHz survey with suitable nuclei. We have examined the radio spectra of all the sources in the survey and selected those which might possibly contain a flat spectrum component stronger than 1 Jy. All of the objects on this short list had suitable high-resolution observations available, from which we were able to tell which sources to include in our sample. Two sources were added to the sample – 3C 147 and 3C 380. The following sources were removed from the sample because their nuclei were too weak: 0600 + 442, 1415 + 463, 1427 + 543, 1636 + 473, 1656 + 482 and 1656 + 571.

Values of r for the sources found to be resolved in the present measurements were taken from the results of the model-fitting described in Section 4. The results of this are given in the last column of Table 1. For a few sources the models are not considered reliable and in these cases r was estimated directly from

$$r = \frac{S_{max} - S_{min}}{S_{max} + S_{min}}$$

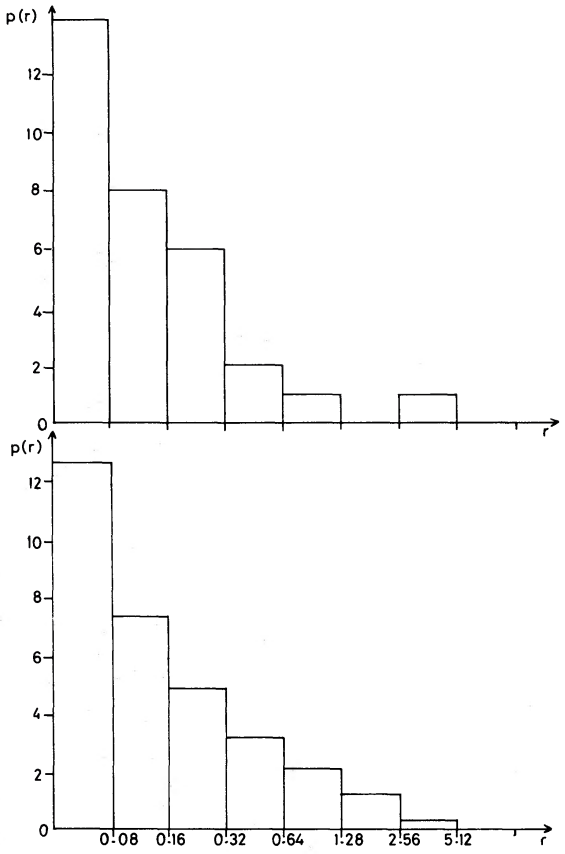

Figure 3. (Upper) The observed distribution of r, the ratio of the flux of the extended component to that of the nucleus.

Figure 4. (Lower) The distribution of r given by the model described in Section 6.

where S_{max} and S_{min} are the maximum and minimum fringe amplitudes observed. These cases are marked with an asterisk in Table 1. The value of r for 3C 147 is well determined and is approximately 4 (Simon *et al.* 1980), while for 3C 380 Wilkinson (private communication) estimates that r is about unity. The distribution $p(r)$ is shown in Fig. 3, where all of the unresolved sources have been put into the lowest bin.

The model which has been used to try to reproduce $p(r)$ is very crude, consisting of similar sources viewed at random orientations. It has the advantage, however, of only four free parameters and, with it, it is possible to produce distributions like that in Fig. 3 to a reasonable degree of accuracy. Thus the model, although crude, is not at variance with observation. Unfortunately it is not possible to specify uniquely the four parameters, since there is more than one acceptable solution. One possible solution is $\gamma_n = 6$, $\gamma_e = 5$, $\phi = 10°$, $r_t = 0.02$ for which $p(r)$ is shown in Fig. 4. The values of γ_n, γ_e and ϕ may be thought to be surprisingly large, γ_n being comparable with what is required to explain the most extreme examples of superluminal expansion (Blandford & Königl 1979). However, these are necessary to broaden $p(r)$ sufficiently to fit the observations. A more realistic model would have distributions in the values of the jet velocities, the intrinsic misalignment and the transverse flux-ratio. These would serve to broaden the distribution, allowing smaller values for the jet parameters.

If the value of γ drops as one moves further from the nucleus, as seems reasonable, then relativistic effects will become less pronounced. In particular the outer structure will be less

Table 3. Summary of source properties. S and F refer to steep or flat low-frequency spectra. The references are for the variability results.

Source	Variable	Spectrum	Resolved	References
0133 + 476	Yes	F	No	1, 2, 3, 5, 9, 10, 11, 12
0316 + 413	Yes	S	Yes	1, 2, 3, 5, 6, 7, 9, 10, 11
0600 + 422	No	S	Yes	
0609 + 607	Yes	S	No	12
0642 + 449	Yes	S	No	9, 12
0707 + 476	Yes	S	No	12
0710 + 439	Yes	F	No	11
0814 + 425	Yes	F	Yes	1, 9, 11, 12
0820 + 560	Yes	S	No	12
0828 + 493	Yes	F	Yes	9, 12
0831 + 557	No	S	Yes	
0850 + 581	No	S	Yes	
0859 + 470	No	S	Yes	
0900 + 428	No	S	Yes	
0945 + 408	No	S	Yes	
0954 + 556	No	S	Yes	
1031 + 567	No	S	No	
1150 + 497	Yes	S	Yes	9, 12
1415 + 463	No	S	Yes	
1418 + 546	Yes	F	No	12
1427 + 543	No	S	Yes	
1624 + 416	Yes	S	No	1, 10
1636 + 473	No	S	Yes	
1642 + 690	No	S	Yes	
1656 + 482	No	S	Yes	
1656 + 571	No	S	Yes	
1738 + 476	No	F	No	
1739 + 522	Yes	F	Yes	12
1749 + 701	Yes	F	No	3, 12
1800 + 440	No	F	Yes	
1807 + 698	Yes	S	Yes	2, 3, 5, 6, 10, 12
1823 + 568	No	S	Yes	
1954 + 513	Yes	S	Yes	11
2200 + 420	Yes	F	No	1, 2, 3, 4, 5, 6, 7, 8, 9, 10, 11, 12
2351 + 456	No	S	Yes	
2352 + 495	Yes	F	Yes	9

References	Frequency (GHz)
1. Altschuler & Wardle (1976)	2.7 and 8.1
2. Andrew *et al.* (1972)	6.7 and 10.6
3. Andrew *et al.* (1978)	6.6 and 10.6
4. Dent & Hobbs (1973)	31.4
5. Dent & Kapitzky (1976)	7.9
6. Dent *et al.* (1974)	15.5
7. Dent & Kojoian (1972)	7.8
8. Fanti *et al.* (1979)	0.4
9. Kesteven *et al.* (1977)	2.7
10. Medd *et al.* (1972)	6.6 and 10.6
11. Webber *et al.* (1976)	1.7
12. This paper	

asymmetric than the nucleus. It is possible that, if γ_e is quite small, weak counter-jets may become visible on the arcsec scale. This would enable γ_e to be measured directly, and low-frequency observations with the MTRLI are now in progress to study this.

It is also possible to extend the predictions of the model and to calculate the expected distribution of misalignment angles between the nucleus and outer component as is observed in several sources (e.g. Readhead *et al.* 1979). This, however, requires better quality observations than those available here. The calculation is outlined in the Appendix and some results are discussed by Browne *et al.* in preparation.

7 Variability and spectral type

Having found those sources with extended emission, it is possible to try to correlate its presence with other properties of the sources such as variability and spectral type. The second column of Table 3 summarizes some results on variability. References 1 to 11 refer to variability studies, while reference 12 indicates those sources whose spectra show a very large scatter, suggesting variability. The spectral classification is on the basis of low-frequency (below 1 GHz) spectral index, α_L, and is given in the third column. Type S sources have relatively steep low-frequency specta ($\alpha_L < 0$), while type F sources have flat or inverted low-frequency spectra ($\alpha_L \geqslant 0$). The fourth column indicates which sources are resolved.

Correlations between resolution, variability and spectral type are presented in Table 4 in the form of contingency tables. The statistical significance of each correlation can be calculated using Fisher's exact probability test (Siegel 1956) which gives the probability of obtaining the observed table, or more extreme ones, if all three properties are uncorrelated. The most striking correlation is that between resolution and variability which has a probability of only 0.6 per cent of occurring by chance. Unresolved sources are very much more likely to be variable than those showing extended emission. Since the variability measurements were made at low angular resolution, it might be thought that the correlation is caused by constant emission from the extended regions diluting a variable flux from the nucleus. However, the extended regions have steep spectra (Davis *et al.* 1977; Perley *et al.* 1980) and contribute a very small fraction of the flux at the high frequencies at which many

Table 4. Correlations between resolution, variability and spectral type in the form of contingency tables.

		Resolved	
		Yes	No
Variable	Yes	8	10
	No	16	2

		Variable	
		Yes	No
Spectrum	S	9	16
	F	9	2

		Spectrum	
		S	F
Resolved	Yes	19	5
	No	9	6

of the variability studies in Table 3 were made. It is thus unlikely that this dilution effect alone can account for the observed correlation in Table 4. Unresolved sources appear to be inherently more variable than the nuclei of resolved sources. The relativistic jet model provides a possible explanation of this since there will be a difference between the observer's time-scale and that for the source. If sources have a range of values of γ_n then those with the largest values will have greatest observed rates of variability and also the greatest amplification of the flux from the nucleus. These sources will have the brightest nuclei, and therefore are the most likely to appear unresolved and are also the most likely to be classified as variable.

The correlations involving spectral type are slightly less clear than that between resolution and variability, but still appear significant. The correlation with variability has a probability of 1.4 per cent of occurring by chance, while that with resolution has a rather higher value of 8 per cent. An interesting feature of them is that they are with low-frequency spectral index (although this is poorly defined for some sources); performing these correlations with high-frequency spectral index yields totally insignificant probabilities. This probably arises because these sources consist of a flat-spectrum nucleus and a steep-spectrum extended component which dominates in the source's total spectrum at low frequencies. Sources with strong extended components are thus resolved and have steep low-frequency spectra.

8 Conclusions

It has been shown that extended emission a few seconds of arc away from the nuclei of flat-spectrum sources is a very common phenomenon. Typically this extended emission has a steep spectrum and constitutes about 10 per cent of the total flux of the source at 1 GHz.

The distribution of component flux-density ratios is in quantitative agreement with the relativistic jet model provided that the outer components are also relativistic. High dynamic range observations at low frequencies are required in order to try to detect any counter-jets in these sources so that γ_e can be measured directly. Work is currently in progress to do this with MTRLI. The relativistic jet model also provides a possible explanation of the correlation found between the absence of extended emission and variability.

The validity of the interpretation of our observations using the relativistic jet model depends on whether bulk relativistic motions can be sustained over hundreds of kpc. At present this is far from clear, but the maps now being made of jets in radio sources should help to answer this question.

References

Altschuler, D. R. & Wardle, J. F. C., 1976. *Mem. R. astr. Soc.*, **82**, 1.
Andrew, B. H., MacLeod, J. M., Harvey, G. A. & Medd, W. J., 1978. *Astr. J.*, **83**, 863.
Andrew, B. H., Medd, W. J., Harvey, G. A. & Locke, J. L., 1972. *Nature*, **236**, 445.
Baars, J. W. M., Genzel, R., Pauliny-Toth, I. I. K. & Witzel, A., 1977. *Astr. Astrophys.*, **61**, 99.
Banhatti, D. G., 1980. *Astr. Astrophys.*, **84**, 112.
Bentley, M., Haves, P., Spencer, R. E. & Stannard, D., 1976. *Mon. Not. R. astr. Soc.*, **176**, 275.
Blandford, R. D. & Königl, A., 1979. *Astrophys. J.*, **232**, 34.
Cohen, A. M., Porcas, R. W., Browne, I. W. A., Daintree, E. J. & Walsh, D., 1977. *Mem. R. astr. Soc.*, **84**, 1.
Conway, R. G. & Stannard, D., 1975. *Nature*, **255**, 310.
Davis, R. J., Stannard, D. & Conway, R. G., 1977. *Nature*, **267**, 596.
Dent, W. A. & Hobbs, R. W., 1973. *Astr. J.*, **78**, 163.
Dent, W. A. & Kapitzky, J. E., 1976. *Astr. J.*, **81**, 1053.
Dent, W. A., Kapitzky, J. E. & Kojoian, G., 1974. *Astr. J.*, **79**, 1232.
Dent, W. A. & Kojoian, G., 1972. *Astr. J.*, **77**, 819.

Fanti, R., Ficarra, A., Mantovani, F., Padrielli, L. & Weiler, K., 1979. *Astr. Astrophys. Suppl.*, **36**, 359.
Gopal-Krishna, 1980. *Astr. Astrophys.*, **86**, L1.
Jenkins, C. J., Pooley, G. G. & Riley, J. M., 1977. *Mem. R. astr. Soc.*, **84**, 61.
Kesteven, M. J. L., Bridle, A. H. & Brandie, G. W., 1976. *Astr. J.*, **81**, 919.
Kesteven, M. J. L., Bridle, A. H. & Brandie, G. W., 1977. *Astr. J.*, **82**, 541.
Longair, M. S. & Riley, J. M., 1979. *Mon. Not. R. astr. Soc.*, **188**, 625.
Medd, W. J., Andrew, B. H., Harvey, G. A. & Locke, J. L., 1972. *Mem. R. astr. Soc.*, **77**, 109.
Miley, G. K., 1971. *Mon. Not. R. astr. Soc.*, **152**, 477.
Perley, R. A., Fomalont, E. B. & Johnston, K. J., 1980. *Astr. J.*, **85**, 649.
Perley, R. A. & Johnston, K. J., 1979. *Astr. J.*, **84**, 1247.
Porcas, R. W., Urry, C. M., Browne, I. W. A., Cohen, A. M., Daintree, E. J. & Walsh, D., 1980. *Mon. Not. R. astr. Soc.*, **191**, 607.
Potash, R. I. & Wardle, J. F. C., 1980. *Astrophys. J.*, **239**, 42.
Readhead, A. C. S., Pearson, T. J., Cohen, M. H., Ewing, M. S. & Moffet, A. T., 1979. *Astrophys. J.*, **231**, 299.
Scheuer, P. A. G. & Readhead, A. C. S., 1979. *Nature*, **277**, 182.
Siegel, S., 1956. *Nonparametric Statistics*, McGraw-Hill.
Simon, R. S., Readhead, A. C. S., Moffet, A. T., Wilkinson, P. N. & Anderson, B. 1980. *Astrophys. J.*, **236**, 707.
Waggett, P. C., Warner, P. J. & Baldwin, J. E., 1977. *Mon. Not. R. astr. Soc.*, **181**, 465.
Wardle, J. F. C., 1978. *Proc. BL Lac Symp.*, ed Wolfe, A. M., University of Pittsburgh Press.
Webber, J. C., De Noyer, L. K., Yank, K. S. & Swenson, G. W., 1976. *Astr. J.*, **81**, 1069.
Weiler, K. W. & Johnston, K. J., 1980. *Mon. Not. R. astr. Soc.*, **190**, 269.

Appendix: Misalignment angles

The intrinsic misalignment, ϕ, between the nucleus and outer component is not the same as the observed misalignment because projection effects are important. Defining the observed misalignment to be the position angle difference between the jet in the nucleus and in the outer component (i.e. the angle between nuclear and outer component extensions), then this is the angle η in Fig. 1. This is given by

$$\cot \eta = \pm (\sin \theta_n \cot \phi \operatorname{cosec} \psi - \cos \theta_n \cot \psi), \tag{A1}$$

where the sign is chosen to give η for the approaching jet. Integration over the distributions of θ_n and ψ (equation 2) enables the distribution of η to be calculated. For the simple model considered here for core-dominated sources, the distribution is a function of only two parameters, γ_n and ϕ and may prove to be a powerful test of the relativistic jet model (Browne *et al.* in preparation).

The results for the model discussed in the previous section are given in Fig. A1. It is remarkable how flat this distribution is for such a small intrinsic misalignment angle ϕ. We

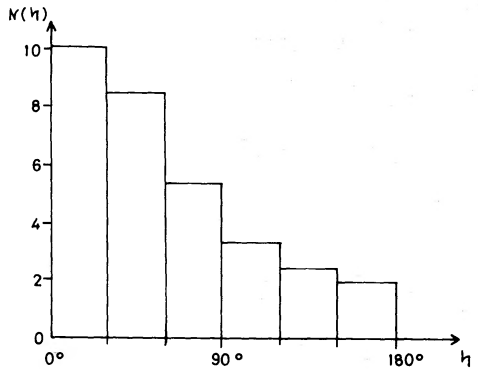

Figure A1. The distribution of η, the misalignment angle in the observer's frame, predicted by the model.

can gain insight into this effect by using the small-angle approximation for θ_n and ϕ. Equation (A1) then becomes

$$\cot \eta = \pm \operatorname{cosec} \psi \left(\frac{\theta_n}{\phi} - \cos \psi \right).$$

Small values of $|\cot \eta|$ are only possible if $\phi > \theta_n$. Consequently, flat distributions of η require $\phi > \theta_{max}$, where θ_{max} is the largest value of θ_n likely to occur (see Fig. 2), and is of order $1/\gamma_n$. Thus large values of η, as observed for some sources (Readhead *et al.* 1979), are quite likely for small values of θ_{max} (i.e. large values of γ_n).